Validation of Turbulence Closures for the RANS Modelling of Under-expanded Fluid Releases

R.M. Woolley[a], M. Fairweather[a], C.J. Wareing[b], and S.A.E.G. Falle[c]

[a]School of Chemical and Process Engineering, University of Leeds, Leeds, LS2 9JT, United Kingdom.
r.m.woolley@leeds.ac.uk
[b]School of Physics and Astronomy, University of Leeds, Leeds, LS2 9JT, United Kingdom.
[c]School of Mathematics, University of Leeds, Leeds, LS2 9JT, United Kingdom.

Abstract. Presented are results from the application of a shock-capturing numerical scheme to the solution of the Favre-averaged Navier-Stokes fluid-flow equations, coupled with compressibility-corrected turbulence models. The relative performance of both a two-equation model and a Reynolds-stress transport model are evaluated in their application to the modelling of both moderately under-expanded, and highly under-expanded experimental releases. Both standard, and compressibility corrected models are investigated, and the superior predictive capabilities of the second-moment Reynolds-stress model are demonstrated.

Keywords: Turbulence modelling; Compressible flow; Second-moment closure; k-ε
PACS: 47.10.ad, 47.11.Df, 47.27.E, 47.40.Hg

INTRODUCTION

The flow-field structure of sub-sonic, perfectly expanded jet releases has been well documented over the years. During this time, a number of descriptive correlations have been obtained which relate the release geometry and fluid properties to the behaviour of the mean flow properties. It has been shown that the decay of the mean fluid volume fraction is proportional to the release diameter, inversely proportional to the square root of the fluid density, and independent of the velocity [1]. Increasing the driving pressure of such a flow will proportionally increase the release velocity until the local speed of sound is reached. At this critical pressure ratio, the maximum velocity is achieved, and any increase in driving force will not increase the velocity. Further pressure increases will however increase the observed release pressure, thus resulting in the fluid expansion occurring downstream from the release aperture, and supersonic fluid flow being observed. The ratio of the reservoir to atmospheric pressure defines whether a jet is moderately under-expanded (1.1 to 2.1) or highly under-expanded (>2.1), the structures displayed in the releases being dependent upon this classification. Such under-expanded jets have a very wide variety of engineering applications including rocket propulsion and maneuvering [2], fuel injection systems [3], and the assessment of consequences and risk assessment of industrial releases [4], in additional to natural occurrences such as during the rapid expansion of volcanic eruption. The ability to accurately predict the detailed structure of such flows requires an understanding and numerical representation of the interaction of turbulent mixing and compressibility effects due to associated phenomena. Presented in this paper are results from a rigorous modelling approach applied to a variety of high-pressure releases, in which turbulence closures are investigated with respect to their efficacy in reproducing experimental observation. Modifications to account for compressibility effects, based upon the most recent theoretical advancements have been incorporated into both two-equation, and second-moment transport models, and comparisons made with standard models. It has been shown recently that previous advances in the modelling of compressible turbulence using a two-equation approach, although proffering improvement in performance over the unmodified model, have been theoretically flawed [5]. Hence, moving forward, it will be required to apply second-moment closures to the prediction of under-expanded flows to ensure a consistent scientific approach, and the sound validation of turbulence models designed to represent compressible fluid phenomena.

NUMERICAL METHOD

The numerical approach to the modelling of the under-expanded jets was based upon the solutions of the Reynolds-averaged, density-weighted forms of the transport equations for mass, momentum, and total energy as described in detail in Woolley et al. [6]. This equation set was closed by the application of a two-equation turbulence model [7] and also a second-moment Reynolds-stress transport model [8]. A number of turbulence sub-models have been investigated, and are further described below.

The two-equation turbulence closure has been extensively used in the prediction of incompressible flows, but is well known to over-predict turbulence levels in under-expanded jets due to not accounting for the turbulence dampening effect of the Joule-Thompson expansion. Observations made of shock-containing flows by Sarkar et al. [9] indicated that the important sink terms in the turbulence kinetic energy budget generated by the shocks were a compressible turbulence dissipation rate, and to a lesser degree, the pressure-dilatation term. In isotropic turbulent flow, the pressure-dilatation term was found to be negligibly small, and so it was proposed that the compressible dissipation rate was introduced as a function of the turbulent Mach number. The application to the k-ε model was then made through modification of the source term for the turbulence energy evolution, and the turbulence viscosity.

A number of possible Reynolds-stress transport approaches for turbulence modelling have been reviewed by Gatski [10], and the most investigated closures centre around the description of the pressure-strain term (A_{ij}) in the descriptive equation (Equation (1)). The pressure-strain term is accountable for the redistribution of the Reynolds stresses, and is now widely accepted as the main contributor to structural compressibility effects [11].

$$\begin{aligned}\frac{\partial}{\partial t}\left(\bar{\rho}u_i''u_j''\right)+\frac{\partial}{\partial x_k}\left(\bar{\rho}u_i''u_j''\tilde{u}_k\right)=C_s\frac{\partial}{\partial x_k}\left(\tau\bar{\rho}u_k''u_l''\frac{\partial}{\partial x_l}u_k''u_l''\right)\\ -\left(\bar{\rho}u_i''u_j''\frac{\partial}{\partial x_k}\left(\tilde{u}_j\right)+\bar{\rho}u_j''u_k''\frac{\partial}{\partial x_k}\left(\tilde{u}_i\right)\right)+A_{ij}-\frac{2}{3}\delta_{ij}\bar{\rho}\varepsilon\end{aligned} \quad (1)$$

The pressure-strain term is typically deconstructed into a 'slow' and 'rapid' part, referring to the rate of response of the terms to changes in the flow-field. Ignoring this 'rapid' element, Rotta [12] modelled the term as Equation (2), which was later extended by Khlifi and Lili [13] to incorporate the effects of compressibility by the introduction of a Mach number dependency, as indicated by Equation (3). Prior to this, Jones and Musonge [8] concentrated upon the

$$A_{ij}=-C_1\varepsilon b_{ij} \quad (2)$$

$$A_{ij}=-C_1\left(1-\beta M_t^2\right)\varepsilon b_{ij} \quad (3)$$

representation of the 'rapid' part which has a fourth-rank tensor as a constituent. The simplest representation of this was given to be that described by Equation (4), where the C_1 term corresponds to the 'slow' part previously discussed. Again, this model was later extended by Gomez and Girimaji [14] by its modification using gradient and

$$\begin{aligned}A_{ij}=-C_1\varepsilon\left(\frac{\bar{\rho}u_i''u_j''}{k}-\frac{2}{3}\delta_{ij}\bar{\rho}\right)+C_2\delta_{ij}\bar{\rho}u_i''u_j''\frac{\partial\tilde{u}_k}{\partial x_l}-C_3P_{ij}+C_4\bar{\rho}k\left(\frac{\partial\tilde{u}_i}{\partial x_j}+\frac{\partial\tilde{u}_j}{\partial x_i}\right)+C_5\bar{\rho}u_i''u_j''\frac{\partial\tilde{u}_l}{\partial x_l}\\ +C_6\left(\bar{\rho}u_k''u_j''\frac{\partial}{\partial x_k}\left(\tilde{u}_k\right)+\bar{\rho}u_k''u_i''\frac{\partial}{\partial x_j}\left(\tilde{u}_k\right)\right)+C_7\bar{\rho}k\delta_{ij}\frac{\partial\tilde{u}_l}{\partial x_l}\end{aligned} \quad (4)$$

turbulent Mach numbers, as defined by Equation (5), and implemented as Equation (6).

$$M_g\equiv\frac{Sl}{a} \quad \text{and} \quad M_t\equiv\frac{\sqrt{2k}}{a} \quad (5)$$

$$A_{ij}=-C_1\left(M_t\right)b_{ij}+\sum_k C_k\left(M_g\right)T_{ij}^k \quad (6)$$

RESULTS AND DISCUSSION

Figure 1 depicts predictions of the normalized centreline axial velocity, plotted against experimental data for a highly under-expanded air jet [15] with a nozzle-pressure ratio of 3.57. As expected, the unmodified k-ε model over-predicts the jet mixing, leading to an over-dissipative solution. The application of a compressible turbulence dissipation rate goes some way to correcting this, as can be seen by the increase in the amplitude and more gradual decay of the decompression-compression cycle evident in the velocity curve. The resolution of the initial shock-laden region remains poor however, and the solution subsequently becomes overly dissipative with downstream

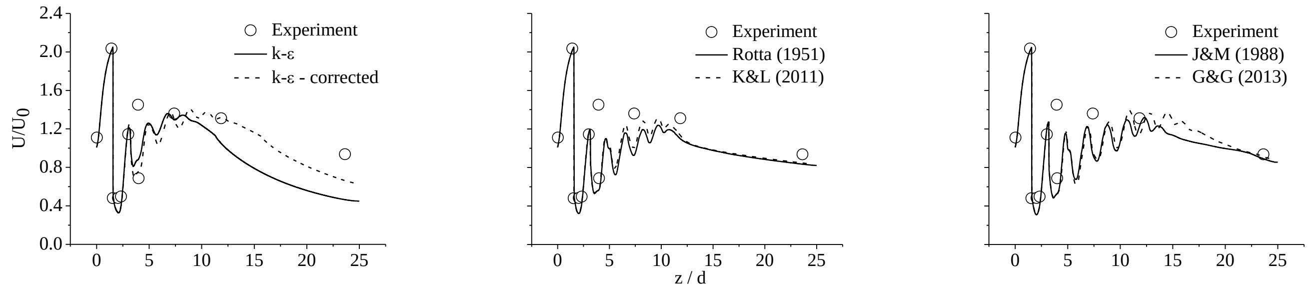

FIGURE 1. Normalised axial velocity predictions (lines) of the highly under-expanded jet plotted against experimental data (symbols) as a function of distance normalised by the nozzle diameter (d).

progression. The Reynolds stress transport model with the closure of the pressure-strain correlation attributed to Rotta [12] notably improves upon the resolution of the shock region and the prediction of the dissipation of turbulence kinetic energy. The introduction of a compressible element to the 'slow' part of the model as discussed by Khlifi and Lili [13] effects an additional increase in peak magnitude predictions in the near field, although has little effect upon the subsequent downstream dissipation. Application of a model for the 'rapid' part of the pressure-strain term [7], incorporated with the model of Rotta for the 'slow' part is a significant improvement with respect to predictions of the shock resolution and the turbulence dissipation. This is again improved by the introduction of corrections based upon the turbulent and gradient Mach numbers reported by Gomez and Girimaji [14].

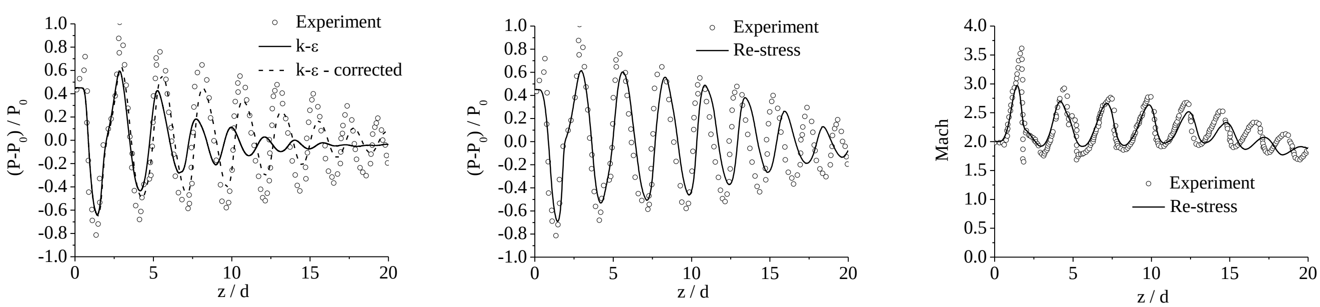

FIGURE 2. Normalised pressure and Mach number predictions (lines) of the moderately under-expanded jet plotted against experimental data (symbols) as a function of distance normalised by the nozzle diameter (d)

Figure 2 depicts normalised pressure predictions plotted against experimental data for the moderately under-expanded air jet of Seiner and Norum [16] with a nozzle-pressure ratio of 1.45. Once again, the k-ε model produces an overly- dissipative solution, which the introduction of a compressible dissipation rate improves upon, increasing the amplitude of the predicted wave, and also bringing the phase more into line with observation. Also shown are pressure predictions obtained using the most successful compressibility-modified Reynolds-stress transport model noted above, which clearly demonstrate the superiority of the approach, maintaining a greater wave amplitude and hence predicting a less-dissipative jet flow. Also shown in Figure 2 are the local Mach number predictions of the moderately under-expanded jet obtained through the application of the modified second-moment model. Although the frequency of the predicted decompression-compression curve conforms well with experimental observation, the spread of the jet is over-predicted from approximately 15 jet diameters onwards. Also, the model fails to predict the magnitude of the first peak, which was also evident in the k-ε model predictions. It can be noted that the behaviour of all the models over the range of the first two cycles are almost identical due to the flow being essentially inviscid in this region.

CONCLUSIONS

The relative performance of a two equation turbulence model and a Reynolds-stress transport model has been evaluated, in the prediction of two under-expanded jets displaying different flow characteristics. The Reynolds-stress transport model has been shown to provide superior predictions of pressures and velocities in both the moderately and highly under-expanded flows. The introduction of a compressible dissipation-rate term to the k-ε model impacts positively upon the model's predictive ability, but this does not show superiority over an unmodified Reynolds-stress transport model. Subsequently, it has been shown that the agreement of the second-moment model with experimental data can be sequentially improved via the application of progressively more complex representations of the pressure-strain term in the transport equation for the modelled Reynolds stress.

NOMENCLATURE

Roman letters:

a	adiabatic sound speed
b	Reynolds-stress anisotropy
k	turbulence kinetic energy
l	length scale
M	Mach number
p	pressure
S	rate of strain tensor
t	time
u	velocity
x, z	spatial dimension

Superscripts:

$\bar{A}$, $\tilde{A}$, A''	Reynolds average/Favre average/fluctuating component

Greek letters:

δ_{ij}	Kronecker delta
ε	dissipation rate of k
ρ	density
τ	turbulence time scale

Subscripts:

g	gradient
i	spatial indice
j	spatial indice
k	spatial indice
t	turbulent
0	reference state

ACKNOWLEDGMENTS

The research leading to the results described herein has received funding from the European Union (E.U.) 7th Framework Programme FP7-ENERGY-2012-1-2STAGE as grant agreement number 309102. The paper reflects only the authors' views and the E.U. is not liable for any use that may be made of the information contained herein.

REFERENCES

1. J.O. Hinze, Turbulence: an introduction to its mechanism and theory, New York: McGraw-Hill, 1959.
2. G. Hagemann, H. Immich, T.V. Nguyen, and G.E. Dumnov. J. Propul. Power **14**(5), 620-634 (1998).
3. T.R. White and B.E. Milton. Shock Waves **18**, 353-364 (2008).
4. R.M. Woolley, M. Fairweather, C.J. Wareing, C. Proust, J. Hebrard, D. Jamois, V.D. Narasimhamurthy, I.E. Storvik, T. Skjold, S.A.E.G. Falle, S. Brown, H. Mahgerefteh, S. Martynov, S.E. Gant, D.M. Tsangaris, I.G. Economou, G.C. Boulougouris, and N.I. Diamantonis. Int. J. Greenh. Gas Con. **27**, 221-238 (2014).
5. W.D. Thacker, S. Sarkar, and T.B. Gatski. Theor. Comp. Fluid. Dyn. **21**, 171-199 (2007).
6. R.M. Woolley, M. Fairweather, C.J. Wareing, S.A.E.G. Falle, C. Proust, J. Hebrard, and D. Jamois. Int. J. Greenh. Gas Con. **18**(1), 139-149 (2013).
7. W.P. Jones and B.E. Launder. Int. J. Heat Mass Tran. **15**(2), 301-314 (1972).
8. W.P. Jones and P. Musonge. Phys. Fluids **31**(12), 3589-3604 (1988).
9. S. Sarkar, G. Erlebacher, M.Y. Hussaini, and H.O. Kreiss. J. Fluid Mech. **227**(1), 473-493 (1991).
10. T.B. Gatski. Theor. Comp. Fluid. Dyn. **18**, 345-369 (2004).
11. S. Sarkar. J. Fluid Mech. **282**, 163-186 (1995).
12. J. Rotta. Z. Phys. A-Hadron. Nucl. **129**, 547-572 (1951).
13. H. Khlifi and T. Lili. JAFM **4**(2), 99-104 (2011).
14. C.A. Gomez and S.S. Girimaji. J. Fluid Mech. **733**, 325-369 (2013).
15. C.D. Donaldson and R.S. Snedeker. J. Fluid Mech. **45**(2), 281-319 (1971).
16. J.M. Seiner and T.D. Norum, "Experiments of Shock Associated Noise on Supersonic Jets", in AIAA 12th Fluid and Plasma Dynamics Conference, AIAA: Williamsburg, Virginia, 1979.